RAPID COMMUNICATIONS

PHYSICAL REVIEW B VOLUME 40, NUMBER 1 1 JULY 1989

Multifractal characteristics of magnetic-microsphere aggregates in thin films

L. J. Huang
Department of Materials Science and Engineering, Tsinghua University, Beijing 100084, China

B. X. Liu
Department of Materials Science and Engineering, Tsinghua University, Beijing 100084, China and Center of Condensed Matter and Radiation Physics, Chinese Center of Advanced Science and Technology (World Laboratory), Beijing, China

J. R. Ding and H. D. Li
Department of Materials Science and Engineering, Tsinghua University, Beijing 100084, China
(Received 28 March 1989)

Iron oxide magnetic-microsphere aggregates observed in thin amorphous films have been characterized by a multifractal measure. It was found that the measure was a nontrivial tool to describe the subtle geometrical features of these fractal patterns and could provide useful information to distinguish the topological differences of the corresponding patterns.

It is accepted at present by most researchers that a fractal dimension alone cannot fully characterize a fractal object. To improve the understanding of the complexity of the kinetics of fractal pattern formation, many efforts have been recently focused on the applications of the harmonic measure (multifractal measure) to quantitatively describe the growth probability distribution (GPD) of a growing fractal, since the GPD mainly determines the long-time structure.[1-8] The multifractal measure reveals that a growing fractal actually consists of a hierarchical nontrivial scaling structure, i.e., a set of power-law singularities,[1] instead of a single fractal dimension. These singularities (represented by α) are generally bound in a range $\alpha_{\min} \leq \alpha \leq \alpha_{\max}$ and the frequency of occurrence of any value of α is measured by the function $f(\alpha)$.[5] The function $f(\alpha)$ can be related to the generalized dimensions $D(q)$ which are sequenced by an infinite q order. If the generalized dimensions $D(q)$ are experimentally available, one can then obtain the $f(\alpha) \sim \alpha$ spectrum by Legendre transformation. The Renyi information dimension[9] and the correlation dimension[3] can be explicitly seen from this measure. These developments in multifractal measure, therefore, provide further information of the geometrical features of a fractal pattern. In this Rapid Communication, we characterize our observed iron oxide aggregates in amorphous films with a multifractal measure. The work is of interest not only because the measure itself can provide some detailed information of the observed patterns, but also because the iron oxide aggregates have been considered to be an important prototype for studying pattern formation. This is because particles interacting via long-range dipolar forces may result in a long-time structure with some specific scaling properties[10] which are quite different from those introduced by the Mullins-Sekerka instability or the diffusion-limited-aggregation (DLA) model.

The iron oxide aggregates were observed in Fe-Cu amorphous films. These alloy films have been prehandled in the following way. The films were first prepared in a sequence of Fe/Cu/Fe/Cu/Fe on cleaved sodium chloride single crystals in a vacuum system by electron-gun evaporation with the total thickness being approximately 60 nm. The specimens were then exposed to 300-keV xenon-ion mixing in an accelerator target chamber. The temperature after the ion bombardment was estimated to be around 300 °C owing to the continuous beam heating. The post-irradiation specimens were submitted to *in situ* annealing in a 200CX transmission electron microscope (TEM) up to a temperature of 825 °C, at which the films were transformed into a metastable crystalline state.[11] The post anneal films were further stored at room temperature for half a year in air and once again examined by TEM. It was found that many iron oxide clusters were randomly distributed in the films after air storage and the structure of the films became amorphous, in close similarity to a spontaneous vitrification process.[12] The clusters formed were confirmed to be iron oxide by comparing the x-ray photoemission spectra of the *in situ* annealed and the air stored samples. The detailed experimentation is not a topic included in this paper.

Two of the iron oxide clusters observed by bright-field TEM are exemplified in Figs. 1(a) and 2(a). The linearities of these clusters are approximately 4–5 μm, while the fine iron oxide microspheres have the linear dimension of 0.05 μm. These dimensions are qualitatively in agreement with those reported in the literature.[10,13] The majority of these clusters are chainlike or open structured, as shown in Fig. 1(a) and the cluster marked a' in Fig. 2(a). However, "compact clusters" like that marked a'' in Fig. 2(a) can also be observed (a similar observation is reported in Refs. 10 and 13). Nevertheless, these compact clusters still exhibit chains locally and can therefore be reckoned to be formed by a similar mechanism, as that of the chainlike open structures, which have been ascribed to be a manifestation of magnetic dipolar interactions.[10]

To calculate the multifractal spectra of these clusters, the key issue is to obtain their GPD. Measurement of the GPD experimentally requires successive pictures of the

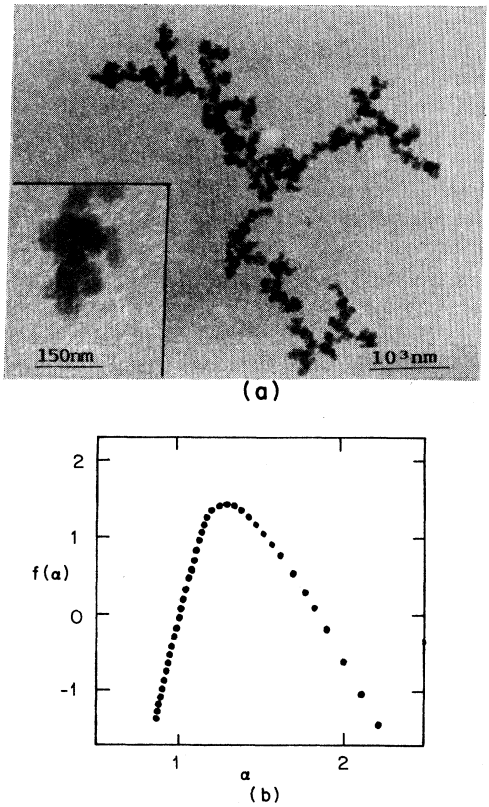

FIG. 1. (a) The TEM micrograph of the iron oxide magnetic microsphere aggregates with the enlarged part showing the stacked spheres, and (b) the corresponding multifractal spectrum.

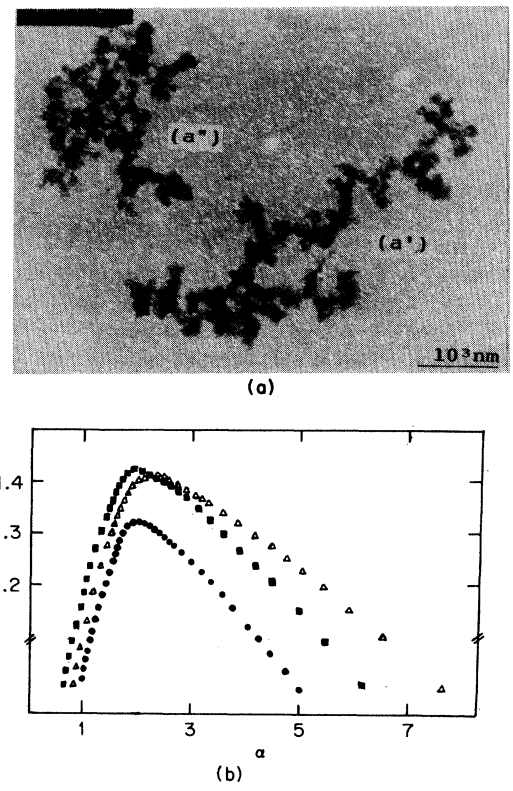

FIG. 2. (a) The TEM micrograph of an open structured aggregate with its neighbor, and (b) their multifractal spectra (see text for details).

growing clusters.[14] However, as a snapshot of the growth process is technically hard to obtain in a solid-state process, the multifractalities of these clusters have to be calculated in an alternative way, i.e., by computer simulations. Several established models, such as DLA and its variations, can be employed to simulate a growth process, but the only way one should follow to describe the growth characteristics of a grown cluster is to put the cluster in a Laplace field, i.e., solve the Laplacian equation numerically, and obtain the corresponding growth probabilities so that the contributions of the fjords (screened parts) are not omitted. This approach has been applied by several authors[7,14] and proved to be efficient and precise by comparison with experimental measurements.[14] The growth probability of a fractal cluster has been accepted to be

$$p_g(\mathbf{r}_s,t) \propto |\nabla_n \phi(\mathbf{r}_s,t)| , \tag{1}$$

where ϕ is the gradient of the potential.

Following the above approach, we first processed the experimentally observed clusters into a two-dimensional square lattice of an image-processing computer with a resolution of 512×512 pixels. The absence of some fine structures of the individual cluster in this procedure can be corrected by coarse graining during calculation and hence the GPD of the cluster obtained should be globally precise.[7] The discrete Laplace equation of the two-dimensional square lattice was solved with the free-boundary condition by the relaxation method. The distance from the center of the cluster to the external boundary is approximately three times the linearity of the cluster as calculated by the authors in Ref. 7. The power-law singularities of the growth probability distribution were calculated by the box counting method with the box size ϵ ranging from 5 to 50 pixels. The generalized dimension $D(q)$ is then obtained by the following definition:[2]

$$D(q) = \lim_{\epsilon \to 0} (q-1)^{-1} \log \left[\sum_i [P_i(\epsilon)]^q \right] / \log \epsilon . \tag{2}$$

The singularity α and function $f(\alpha)$ were obtained by Legendre transformation of q and $D(q)$.

Table I lists the key parameters obtained in this calculation for the clusters exhibited in Figs. 1(a) and 2(a).

TABLE I. List of the key parameters of the multifractal spectra in Figs. 1(b) and 2(b).

	Cluster 1(a)	Cluster 2(a)	Cluster 2(a')	Cluster 2(a'')
$D(0)$	1.40±0.05	1.41±0.05	1.31±0.05	1.43±0.05
$D(1)$	1.04±0.05	0.90±0.05	0.96±0.05	1.01±0.05
$D(2)$	0.92±0.05	0.86±0.05	0.92±0.05	0.82±0.05
α_{min}	0.84±0.05	0.83±0.05	0.90±0.05	0.77±0.05
α_{max}	2.02±0.05	7.69±0.05	5.12±0.05	6.29±0.05

These parameters include the fractal dimension of the support of the probability measure (the fractal dimension of the cluster) $D(0)$, the information dimension $D(1)$, the correlation dimension $D(2)$, the leading singularities $\alpha_{\min}$, and the singularities of the scaling at the enclosed regions (the deepest fjords) $\alpha_{\max}$. Figures 1(b) and 2(b) present the $f(\alpha)$ spectra of the respective clusters shown in Figs. 1(a) and 2(a). The values of the column denoted as cluster 2(a)-2(a'') are the ones calculated by taking the two clusters shown in Fig. 2(a) as a whole [cluster 2(a)] and separately [cluster 2(a') and cluster 2(a'')], as marked in the figure.

From Table I, one sees that all these parameters quantitatively reflect the subtle geometrical differences of these clusters. The numerical values of the fractal dimension $D(0)$ of all these clusters are in quantitative agreement with those obtained by computer simulation with a dipolar interaction and with the experimental results of cobalt aggregates.[10,13] Concerning the individual characteristics of the two clusters shown in Fig. 2(a), it is of interest that the values of $D(0)$ of these two clusters are remarkably different. The chainlike cluster (a') has a much smaller fractal dimension [$D(0)=1.31$] than the compact cluster [$D(0)=1.43$]. This diversity could be interpreted as due to the different strength of the dipolar interactions during the growth of the clusters. Although these differences of their fractal dimensions imply that their geometrical features are diverse, further information is nevertheless last. Also, if taking the two clusters in Fig. 2(a) as a whole (this calculation is relevant since the physical realm makes these two clusters strongly interact with each other), the combination has the same fractal dimension as the cluster in Fig. 1(a), and approximately the same as the cluster (a'') within the experimental error.

Therefore, the result explicitly shows that the fractal dimension alone cannot fully characterize the detailed geometrical features of these clusters, which, however, can be elucidated from the other parameters listed in Table I. The information dimension $D(1)$ reflects the characteristics of the unscreened surfaces (the active zone) of the clusters. Its theoretical value [$D(1)=1$ in two dimensions] has been obtained by Matsushita *et al.* and is thought to be independent of the fractal dimension of the global pattern.[6,15] The $D(1)$ obtained here agrees with the theory and indeed has the same unit value within the experimental error, except in the case when two clusters, (a') and (a''), are taken as a whole. The results, therefore, indicate that the active zones of all these clusters followed the same scaling power law which implies that the growth mechanism might be universal in the present case. When the two clusters, (a') and (a''), were taken as a whole, however, the region between the two clusters became "screened" (the Laplacian potential in this region is very weak). The active zone then became more localized (diminished) resulting in a decrease of the dimension. The information dimension thus provides one subtle geometrical difference that the fractal dimension cannot distinguish.

The correlation dimension $D(2)$ stands for the chance that two arbitrary points of the cluster have a distance $l_i \leq \epsilon$ where ϵ is the size of the counting box employed. The results (see Table I) show that the chainlike or stringy structures possess a larger correlation dimension. This geometrical difference of the clusters means that the open structures have fewer screened parts and hence a denser point-to-point distribution. The major discrepancy between our present results and the theory[4,16] is the value of the leading singularities $\alpha_{\min}$. The "large-wedge" model[4] predicts that $D(0)=1+\alpha_{\min}$. In our case, the $\alpha_{\min}$'s are all too large to fit this prediction. There are two possible reasons for this discrepancy. On one hand, the large wedge model may not perfectly predict the growth process with long-range dipolar interactions which require a more strongly orientated growth than the off-lattice DLA model does. On the other hand, the cluster here might not be fully matured, for the primary growth form can have a much larger leading singularity than the matured ones do.[17] The range of the singularities [see also Figs. 1(b) and 2(b)] is another geometrical parameter which quantitatively reflects the proportion of the screened parts (the enclosed regions) of the cluster. The smaller the $\alpha_{\max}$ is, the more open or more homogeneous the structure will be. In other words, those structures will have fewer singularities.

Another interesting issue is to compare the cluster shown in Fig. 1(a) and the a' in Fig. 2(a). Their fractal dimensions are the same within the experimental error (see Table I). Moreover, since these two clusters were produced in the same film and by the same mechanism, these two clusters should be invariant under topological transformation, i.e., they should be homeomorphic.[18] However, their multifractal spectra [see Figs. 1(b) and 2(b)] are quite different in the range of the singularities. This indicates that they may belong to different universality classes.[18] This contradiction implies that these two clusters can never be smoothly transformed into each other.

In conclusion, we show that each parameter of the multifractal approach provides the subtle geometrical difference of a fractal cluster independently, and the fractal dimension alone can hardly distinguish such geometrical characteristics of a fractal cluster. We also note that the information provided by these parameters is nontrivial for providing a full geometrical knowledge of a fractal object, although each representation of the fractal boundary concerned may not itself be geometrically fractal.[19,20]

The authors acknowledge stimulating communications with Wu Xiaozhong of the James Franck Institute, University of Chicago. This work is partly supported by the Research Fund of Tsinghua University, the National Natural Science Foundation of China, and the International Atomic Energy Agency (Research Contract No. 4731/RB). The assistance of the staff of the TEM Laboratory of Beijing University is also acknowledged.

[1]T. C. Halsey *et al.*, Phys. Rev. A **33**, 1141 (1986).
[2]H. G. H. Hentschel and I. Procaccia, Physica D **8**, 435 (1983).
[3]P. Grassberger and I. Procaccia, Physica D **13**, 34 (1984); **9**, 189 (1983); Phys. Rev. Lett. **50**, 346 (1983).
[4]T. C. Halsey, P. Meakin, and I. Procaccia, Phys. Rev. Lett. **56**, 854 (1986).
[5]I. Procaccia and R. Zeitak, Phys. Rev. Lett. **60**, 2511 (1988).
[6]M. Matsushita *et al.*, Phys. Rev. Lett. **59**, 86 (1987).
[7]Y. Hayakawa, S. Sato, and M. Mutsushita, Phys. Rev. A **36**, 1963 (1987).
[8]C. Amitrano, A. Coniglio, and F. di Liberto, Phys. Rev. Lett. **57**, 1016 (1986).
[9]A. Renyi, *Probability Theory* (North-Holland, Amsterdam, 1970).
[10]G. Helgesen *et al.*, Phys. Rev. Lett. **61**, 1736 (1988); P. M. Mors, R. Botet, and R. Jullien, J. Phys. A **20**, L975 (1987).
[11]L. J. Huang *et al.* (unpublished).
[12]M. Allmen and A. Blatter, Appl. Phys. Lett. **50**, 1873 (1987).
[13]G. A. Niklasson *et al.*, Phys. Rev. Lett. **60**, 1735 (1988).
[14]S. Ohta and H. Honjo, Phys. Rev. Lett. **60**, 611 (1988).
[15]N. G. Makarov, Proc. London Math. Soc. **51**, 369 (1985).
[16]L. P. Turkevich and H. Scher, Phys. Rev. Lett. **55**, 1026 (1985).
[17]P. Ramanlal and L. M. Sander, J. Phys. A **21**, L995 (1988).
[18]A. Arneodo and M. Holschneider, J. Stat. Phys. **50**, 599 (1988).
[19]M. Blunt and R. C. Ball, in *Fractal Aspects of Materials,* edited by D. A. Weitz, L. M. Sander, and B. B. Mandelbrot (Materials Research Society, Pittsburgh, 1988), Vol. EA-17, p. 115.
[20]P. Alstrom, in Ref. 19, p. 119.

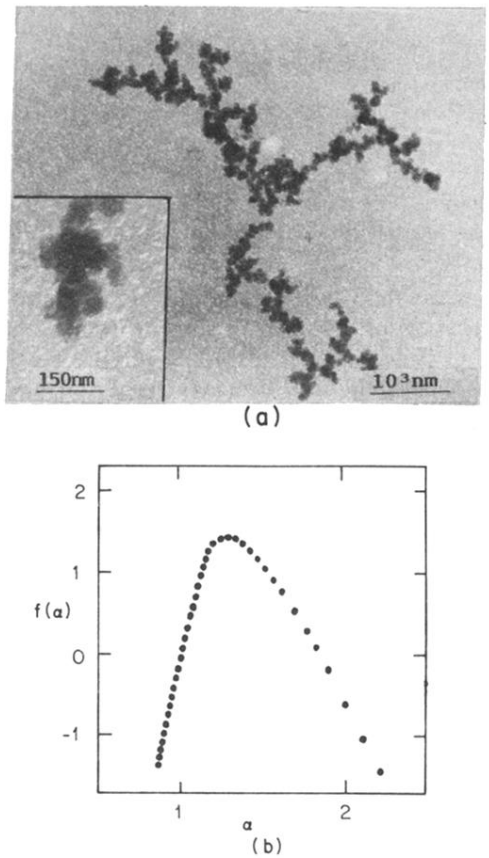

FIG. 1. (a) The TEM micrograph of the iron oxide magnetic microsphere aggregates with the enlarged part showing the stacked spheres, and (b) the corresponding multifractal spectrum.

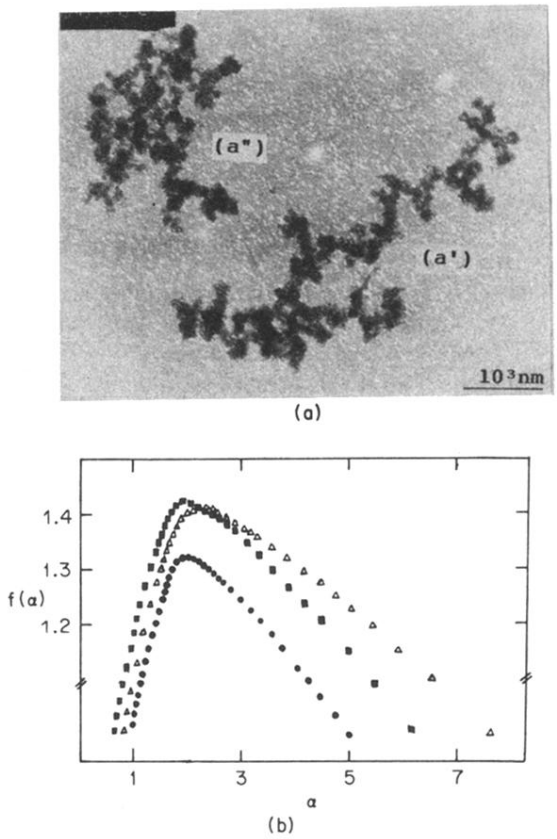

FIG. 2. (a) The TEM micrograph of an open structured aggregate with its neighbor, and (b) their multifractal spectra (see text for details).